Phase Relations and Elemental Distributions in the Ceramics of the Pseudo-Binary Systems $CaZrTi_2O_7 – LnAlO_3$ (Ln = Eu, Gd)

N.S. Mikhailenko, S.V. Stefanovsky
SIA Radon, 7th Rostovskii lane 2/14, Moscow 119121 Russia

A.V. Ochkin
D. Mendeleev University of Chemical Technology, Miusskaya sq. 9, 125047 Russia

M.I. Lapina
IGEM RAS, Staromonetniy 35, Moscow, 109117 Russia

ABSTRACT

Zirconolite and perovskite were found to be major and minor phases respectively in the ceramics of the series (1-*x*) $CaZrTi_2O_7 – x\ EuAlO_3$ and (1-*x*) $CaZrTi_2O_7 – x\ GdAlO_3$ (*x* = 0.25; 0.5; 0.75) produced by cold pressing and sintering at 1400, 1450 and 1500 ^{0}C. Zirconolite and cubic fianite-type oxide (in the Eu-bearing ceramics) were extra phases. At *x* = 0.25 major host phase for Eu and Gd is zirconolite accumulating of up to 90% of total Eu and Gd. With increase *x* value to 0.5 zirconolite remains major host phase for both Eu and Gd and accommodates almost 70% of total Eu_2O_3 and about 60% of total Gd_2O_3. Perovskite becomes major phase for both Eu_2O_3 and Gd_2O_3 at *x* = 0.75 accumulating of about 66% of total Gd_2O_3. As follows from SEM/EDS data Eu and Gd contents in the zirconolite may exceed ~1 formula units, therefore, zirconolite ceramics may be effective matrices for actinide fraction of HLW where Am and Cm are dominant because their crystal chemical behavior is similar to behavior of Gd.

INTRODUCTION

Minor europium and gadolinium (few percents) are present in the rare earth-actinide (REE/An) fraction of high level waste (HLW) [1]. Nevertheless, a study of their behavior at immobilization in ceramics is rather important because Gd is normally considered as trivalent plutonium and curium surrogate as well as neutron absorber to be presented in the zirconolite- and pyrochlore-based ceramics for excess weapons plutonium immobilization [2,3]. Along with zirconolite and pyrochlore major host phases for the Gd and actinides are considered to be perovskite, monazite, and apatite [4]. We suggested zirconolite-perovskite associations to immobilize REE/An fraction of HLW [5], therefore a study of behavior of REEs and actinides in these matrices is required. No reference data on Eu-bearing zirconolites were found. Incorporation of Gd in the zirconolite is studied in details [4,6-10]. Isomorphic capacity with respect to Gd was found to be 1.4 formula units (fu) [4], i.e. Gd^{3+} ions are capable to substitute for Ca^{2+} ions completely by the scheme of $Ca^{2+} + Ti^{4+} = Gd^{3+} + Me^{3+}$ (Me = Al, Fe) and up to 40% Zr^{4+} by epy scheme $Zr^{4+} + Ti^{4+} = Gd^{3+} + Me^{5+}$ (Me = Nb, Ta). At that, in the compositional series $Ca_{1-x}Gd_xZrTi_{2-x}Me^{3+}{}_xO_7$ increase of the *x* value transforms monoclinic structure (zirconolite-2M) to trigonal (zirconolite-3T) or orthorhombic (zirconolite-3O) or at different substitutions – to pyrochlore structure ($Gd_2Ti_2O_7$).

Gadolinium aluminate $GdAlO_3$ is isostructural with calcium titanate $CaTiO_3$ (perovskite). They both have orthorhombic lattice symmetry (space group *P*nma) and form continuous solid solution [11]. The same is expected to be for $EuAlO_3$ with the same space group (JCPDS-ICDD 9-84).

The present works continues a series of our works on investigations of phase relations in pseudo-binary systems: zirconolite – lanthanide aluminate (perovskite) [12-14] and describes phase relations in some ceramics related to the $CaZrTi_2O_7$-$EuAlO_3$ and $CaZrTi_2O_7$-$GdAlO_3$ systems. Some preliminary results were reported in ref. [15].

EXPERIMENTAL

Ceramic samples with specified compositions (1-*x*) $CaZrTi_2O_7$ – *x* $EuAlO_3$ and (1-*x*) $CaZrTi_2O_7$ – *x* $GdAlO_3$ (*x* = 0.25, 0.5 and 0.75) were studied. Oxide mixtures were milled, mechanically activated and homogenized in a planetary mill AGO-2U, compacted in pellets 5 mm in diameter and 2 mm in height, followed by heat-treatment of the pellets in a resistive furnace stepwise to target sintering temperature (1400, 1450 or 1500 ^{0}C), holding at this temperature for 5 hours, and cooled down to room temperature in a turned-off furnace.

The samples were examined with X-ray diffraction using a Philips diffractometer and scanning electron microscopy with energy dispersive system (SEM/EDS) using a JSM-5300+Link ISIS analytical unit. Results of quantitative EDS analyses were recalculated to oxides assuming conventional valence states for Ca, Al, Ti, Zr, Gd, and O. Concentration of elemental europium to oxide was recalculated assuming its di- or trivalent state depending on charge balance.

RESULTS AND DISCUSSION

The Eu-doped ceramics with low content of perovskite constituent (*x* = 0.25) sintered at 1400, 1450, and 1500 ^{0}C have the same phase composition and consist of about 90-95% zirconolite and 5-10% perovskite (Figure 1). SEM images in backscattered electrons demonstrate zirconolite as major light-gray colored bulk and perovskite – as dark-gray inclusions (Figure 2). Chemical compositions of the phases (Table I) are recalculated well to formulae (1450 ^{0}C): $Ca_{0.76}Eu_{0.30}Zr_{1.04}Ti_{1.63}Al_{0.27}O_7$ (zirconolite) and $Ca_{0.80}Eu_{0.16}Zr_{0.06}Ti_{0.90}Al_{0.08}O_3$ (perovskite). Charge balance shows that major Eu in the perovskite is present as Eu(II).
If in oxide mixtures with low Eu and Al contents (*x* = 0.25) phase formation reactions are completed at temperatures below 1400 ^{0}C then at their higher content (*x* = 0.50 and *x* = 0.75) residual baddeleyite is still present at 1400 ^{0}C (Figure 1) and this phase disappears completely only in the samples sintered at 1450 and 1500 ^{0}C. Samples with *x* = 0.5 sintered at these temperatures are composed of major zirconolite (75-80% of total bulk) and minor perovskite (20-25%) – see Figures 1 and 2. Zirconolite grains on SEM-images are some darker than those of perovskite (Figure 2). Their chemical compositions (Table I) in the ceramics sintered at 1500 ^{0}C correspond to formulae: $Ca_{0.46}Eu_{0.64}Zr_{1.16}Ti_{1.28}Al_{0.47}O_7$ (zirconolite) and $Ca_{0.63}Eu_{0.37}Zr_{0.02}Ti_{0.69}Al_{0.27}O_3$ (perovskite). In the ceramic sintered at 1450 ^{0}C grain size of these phases is 1 μm and lower therefore chemical composition of individual phases cannot be

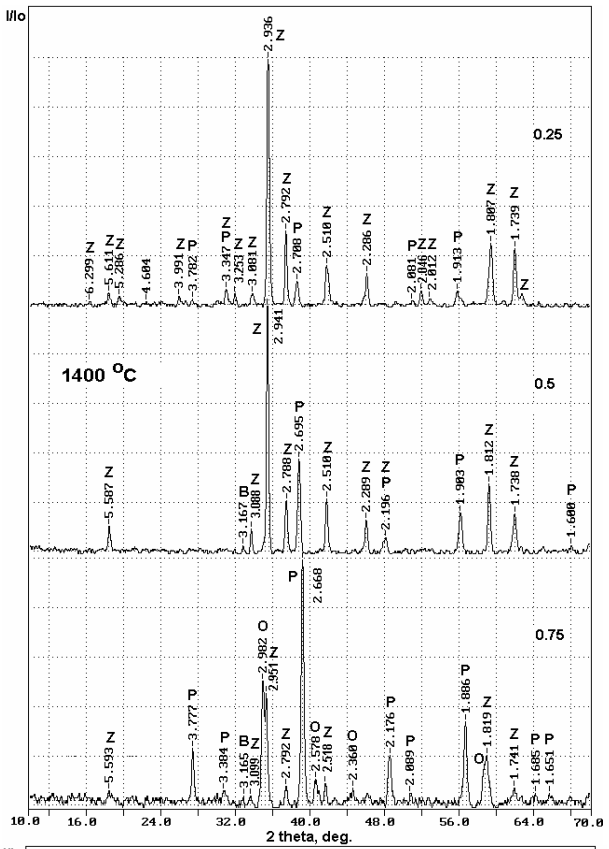

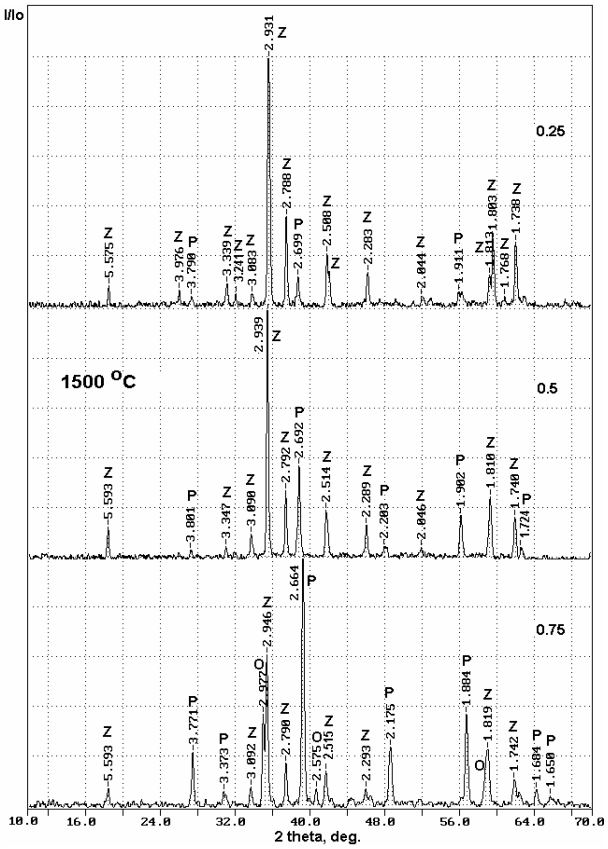

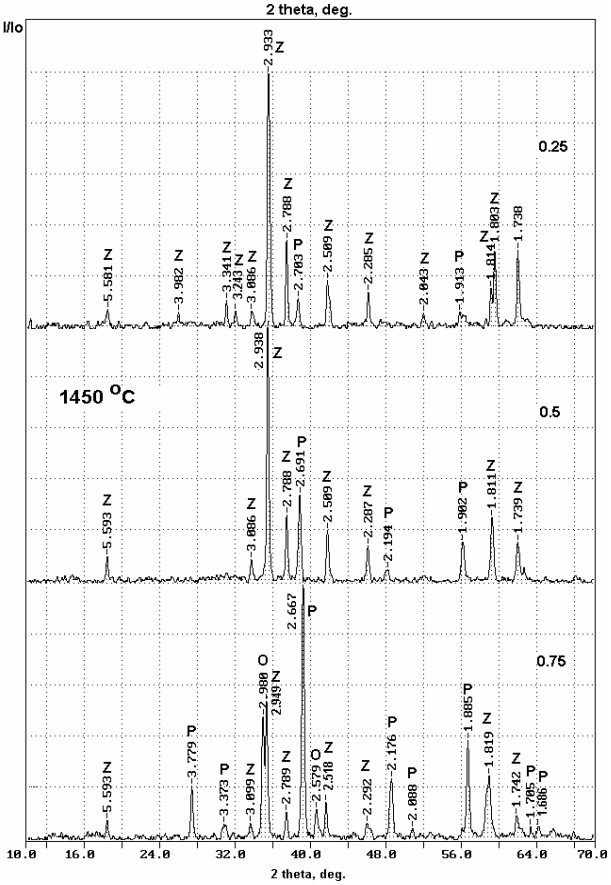

Figure 1. XRD patterns of the ceramics in series (1-*x*) $CaZrTi_2O_7$ – *x* $EuAlO_3$ prepared by sintering at various temperatures.

O – oxide phase (fianite), P – perovskite structure phase, Z – zirconolite.

Table I. Chemical Compositions (wt.%) of the Phases in Eu and Gd Bearing Ceramics.

Oxides	x = 0.25, 1450 ^{0}C		x = 0.5, 1450 ^{0}C		x = 0.5, 1500 ^{0}C		x = 0.75, 1450 ^{0}C			
	Z	P	P+Z	F	Z	P	1(oxide)	2	3	4
Al_2O_3	3.73	2.51	12.06	0.4	5.93	7.86	1.42	8.48	13.39	7,99
CaO	11.63	28.52	6.98	1.55	6.40	20.05	2.05	6.66	7.27	4,09
TiO_2	35.34	45.87	14.75	2.85	25.37	31.01	9.41	12.59	14.95	9,61
ZrO_2	34.91	4.55	9.61	68.52	35.48	1.36	42.45	15.00	8.24	12,55
Eu_2O_3	14.39	17.21	54.22	29.54	28.20	37.36	45.71	58.46	56.56	63,44
Total	100.00	98.66	97.62	102.86	101.38	97.64	101.05	101.19	100.41	97,68

	x = 0.25, 1450 ^{0}C		x = 0.5, 1450 ^{0}C			x = 0.5, 1500 ^{0}C		x = 0.75, 1450 ^{0}C	
	Z	P	Z	P	F	Z	P	Z	P
Al_2O_3	3.73	2.40	7.83	15.38	0.39	6.65	8.65	0.26	10.84
CaO	10.87	26.60	3.39	7.93	1.30	5.56	17.27	1.24	6.04
TiO_2	36.34	47.85	19.85	15.52	3.89	25.14	30.69	3.555	17.89
ZrO_2	33.68	4.15	29.85	2.97	62.58	34.58	1.80	61.36	14.52
Gd_2O_3	14.35	18.39	40.15	56.53	32.21	27.34	39.34	31.445	49.60
Total	98.97	99.39	101.07	98.33	100.37	99.27	97.75	97.86	98.89

F – fluorite structure oxide, P – perovskite-type phase, Z – zirconolite, 1-4 – analytical points on Figure 2.

determined precisely with the exception of Eu-stabilized cubic zirconia (fianite) whose grains may reach 5-7 μm in size. Its averaged formula is $Eu_{0.21}Zr_{0.71}Ti_{0.04}Ca_{0.03}Al_{0.01}O_{1.86}$.

In the ceramics with x = 0.75 perovskite becomes major phase and zirconolite and fianite are minor phases (Figure 1). As follows from XRD and SEM data amounts of the phases may be estimated as ~50% perovskite, 25-30% zirconolite, and 20-25% fianite. Due to small zirconolite grain size (1-2 μm) EDS measurements give wide compositional variations: $Ca_{0.36…0.52}Eu_{1.48…1.76}Zr_{0.52…0.56}Ti_{0.60…0.72}Al_{0.76}O_{7-x}$ ($Ca_{0.44}Eu_{1.52}Zr_{0.58}Ti_{0.70}Al_{0.76}O_{6.42}$ on average). Formulae of the perovskite and fianite phases having larger grains are $Ca_{0.26}Eu_{0.66}Ti_{0.38}Zr_{0.14}Al_{0.54}O_3$ and $Eu_{0.33}Zr_{0.44}Ti_{0.15}Ca_{0.05}Al_{0.03}O_{2-x}$, respectively.

Phase formation reactions in the system with low (x = 0.25) and middle (x = 0.5) Gd and Al content are completed at temperatures below 1400 ^{0}C and ceramics are composed of zirconolite (90-95% and 70-75%< respectively) and perovskite (5-10% and 25-30%, respectively). In the system with high content of perovskite constituent (x = 0.75) reactions are completed within the temperature range between 1400 ^{0}C and 1450 ^{0}C. In the ceramic sintered at 1400 ^{0}C except perovskite (50-55%) and zirconolite (~15%) oxide phase (~30%) was present. Sintering at higher temperatures almost eliminated it and ceramics were composed of only perovskite and zirconolite (Figure 3). XRD patterns exhibit amounts of these phases as 50-55% and 40-45% (at 1450 ^{0}C) and ~60% and ~40% (at 1500 ^{0}C), respectively.

SEM-image of the Gd-containing ceramic with x = 0.25 sintered at 1450 ^{0}C demonstrates major light-gray colored zirconolite bulk with dark-gray zirconolite inclusions (Figure 4). Chemical compositions of the phases are recalculated well to formulae: $Ca_{0.72}Gd_{0.28}Zr_{1.00}Ti_{1.68}Al_{0.28}O_7$

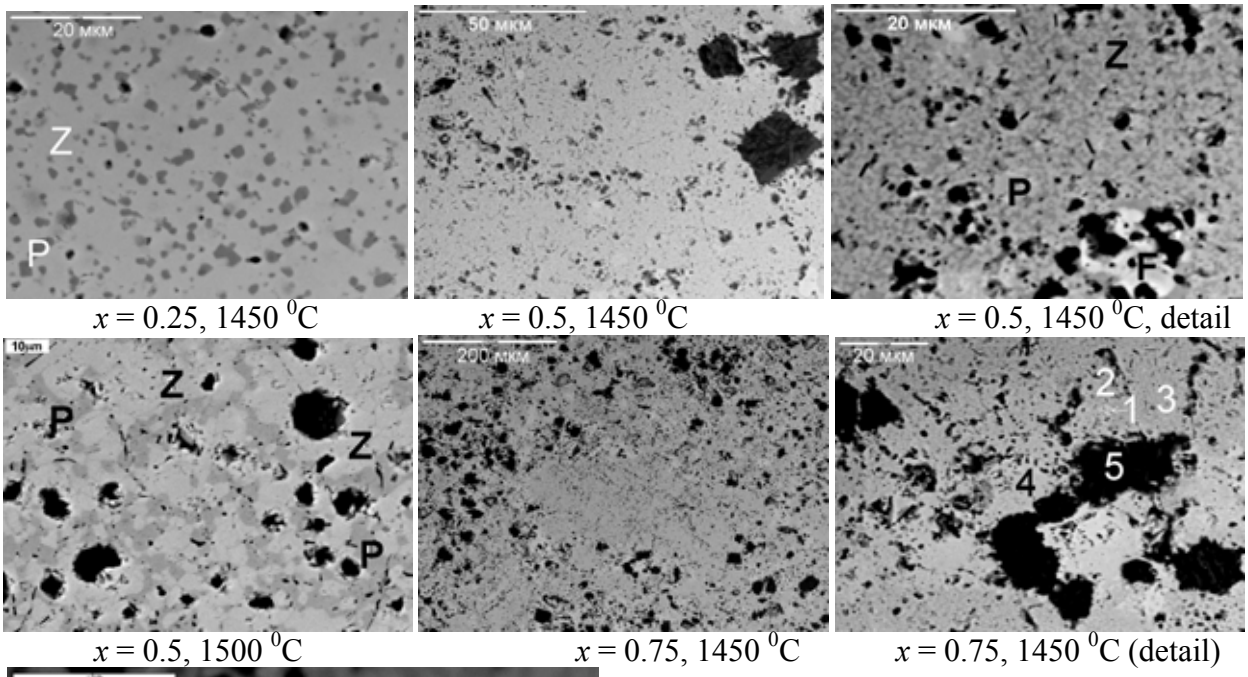

x = 0.25, 1450 ^{0}C | *x* = 0.5, 1450 ^{0}C | *x* = 0.5, 1450 ^{0}C, detail

x = 0.5, 1500 ^{0}C | *x* = 0.75, 1450 ^{0}C | *x* = 0.75, 1450 ^{0}C (detail)

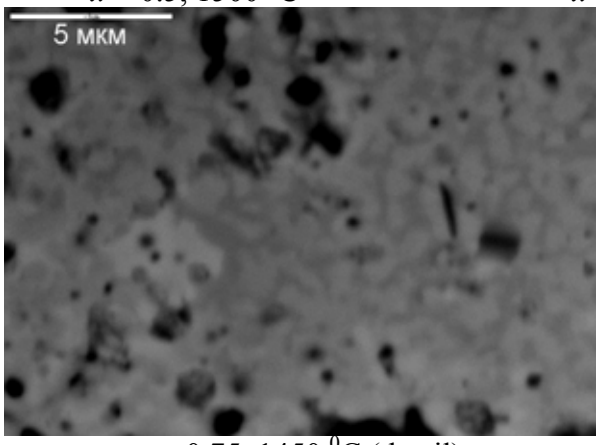

x = 0,75, 1450 ^{0}C (detail)

Figure 2. Backscattered SEM-images of the ceramics in series (1-x) $CaZrTi_2O_7$ – x $EuAlO_3$ prepared by sintering at various temperatures

O – oxide phase (fianite), P – perovskite structure phase, Z – zirconolite.

Digits on photo *x* = 0.75, 1450 ^{0}C (detail) correspond to analytical points in Table I.

(zirconolite) and $Ca_{0.76}Gd_{0.14}Zr_{0.05}Ti_{0.95}Al_{0.07}O_3$ (perovskite). Zirconolite composition is rather constant whereas perovskite exhibits appreciable compositional variations. Texture of the ceramic with *x* = 0.5 sintered at 1450 ^{0}C looks like gray-colored fine-grained bulk containing lighter fianite inclusions with variable grain size. At higher magnification there are variations in color of major bulk due to occurrence of sub-micron-sized zirconolite (darker) and perovskite (lighter) crystals. Chemical composition (Table I) of zirconolite and perovskite may be recalculated to averaged formulae $Ca_{0.26}Gd_{0.98}Zr_{1.04}Ti_{1.08}Al_{0.68}O_7$ and $Ca_{0.28}Gd_{0.66}Ti_{0.40}Al_{0.60}Zr_{0.04}O_3$, respectively. However, due to very fine grain size of both phases these formulae more than likely exhibit chemical composition of microcrystalline aggregates. The only averaged fianite formula $Gd_{0.23}Zr_{0.67}Ti_{0.07}Ca_{0.03}O_{1.86}$ may be determined reliably. In the ceramic sintered at 1500 ^{0}C size of zirconolite and perovskite crystals reaches 5-10 μm across and chemical composition of the phases is more accurate and may be recalculated to formulae: $Ca_{0.41}Gd_{0.61}Zr_{1.15}Ti_{1.29}Al_{0.53}O_7$ (zirconolite) and $Ca_{0.54}Gd_{0.40}Zr_{0.03}Ti_{0.68}Al_{0.30}O_3$ (perovskite).

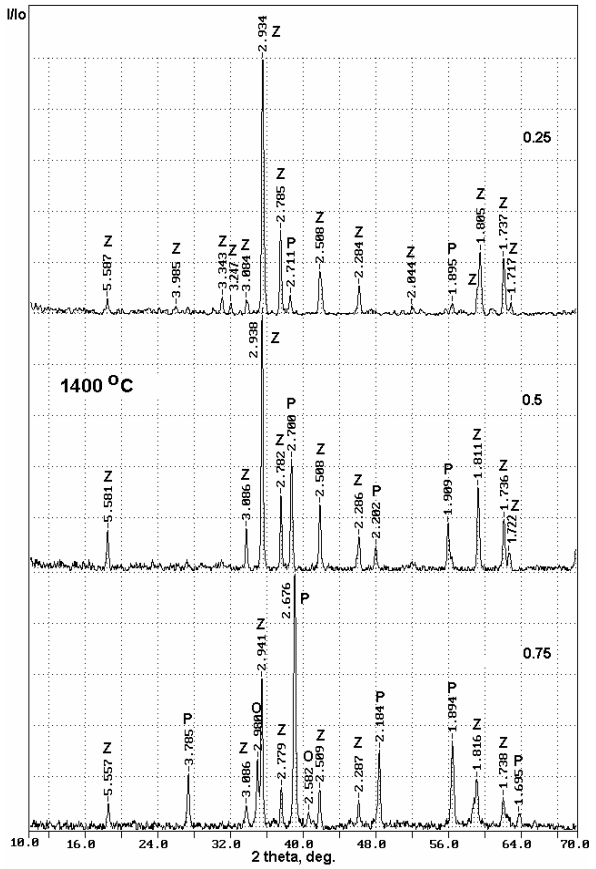

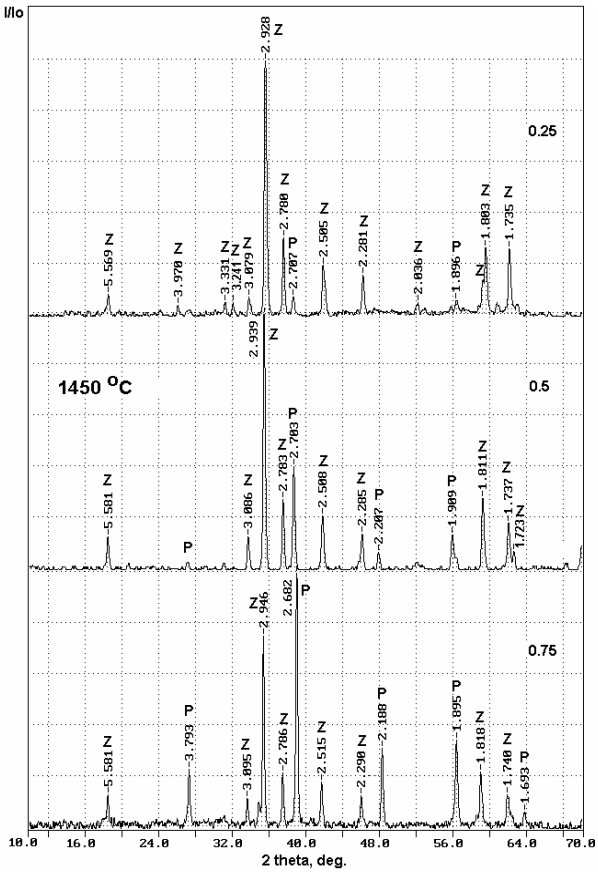

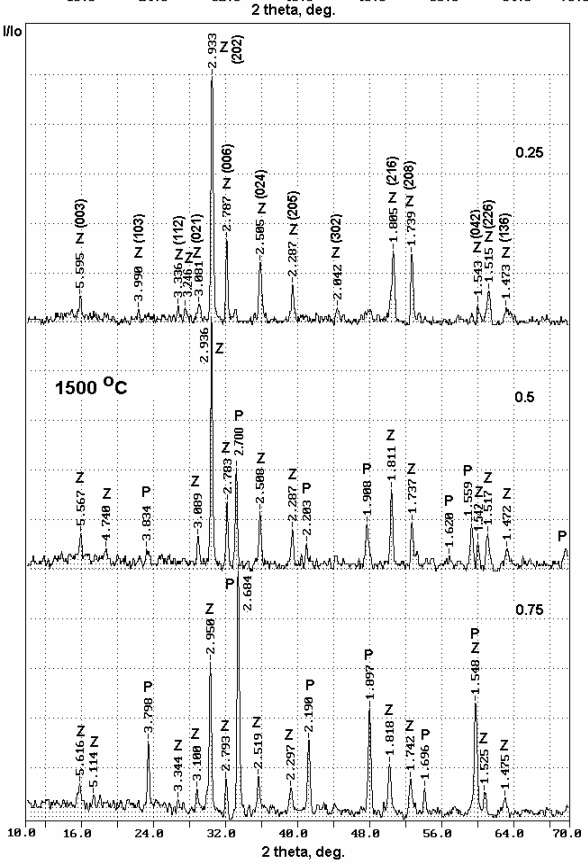

Figure 3. XRD patterns of the ceramics in the series (1-x) $CaZrTi_2O_7$ – x $GdAlO_3$ prepared by sintering at various temperatures.

O – oxide phase (fianite), P – perovskite structure phase, Z – zirconolite.

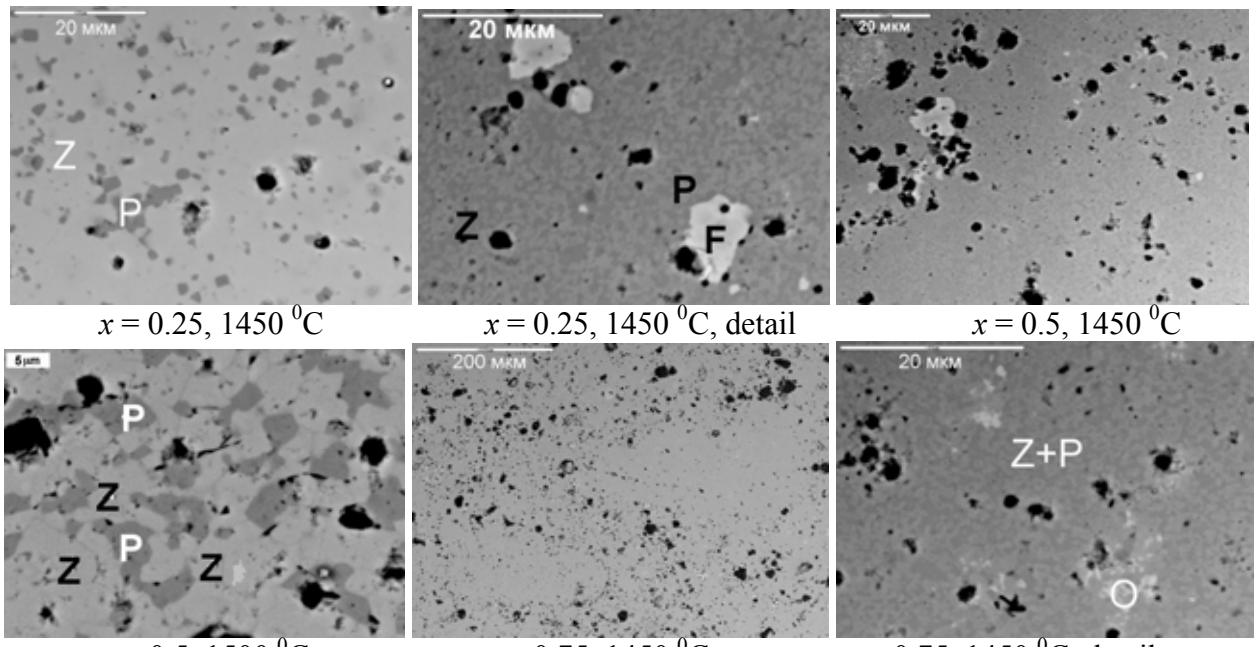

x = 0.25, 1450 ^{0}C | x = 0.25, 1450 ^{0}C, detail | x = 0.5, 1450 ^{0}C

x = 0.5, 1500 ^{0}C | x = 0.75, 1450 ^{0}C | x = 0.75, 1450 ^{0}C, detail

Figure 4. Backscattered SEM-images of the ceramics in series (1-x) $CaZrTi_2O_7$ – x $GdAlO_3$ prepared by sintering at various temperatures

O – oxide phase (fianite), P – perovskite structure phase, Z – zirconolite.

Table II. Waste Oxides Partitioning among Co-existing Phases.

(1-x) $CaZrTi_2O_7$ – x $EuAlO_3$								
T, ^{0}C	x	Phase	Fraction, %	Al_2O_3	CaO	TiO_2	ZrO_2	Eu_2O_3
1450	0.25	Zirconolite	90	93	78	87	99	88
		Perovskite	10	7	22	13	1	12
1500	0.5	Zirconolite	75	69	48	71	99	69
		Perovskite	25	31	52	29	1	31
(1-x) $CaZrTi_2O_7$ – x $GdAlO_3$								
T, ^{0}C	x	Phase	Fraction, %	Al_2O_3	CaO	TiO_2	ZrO_2	Gd_2O_3
1450	0.25	Zirconolite	90	93	79	87	99	87
		Perovskite	10	7	21	13	1	13
1500	0.5	Zirconolite	70	65	43	66	98	62
		Perovskite	30	35	57	34	2	38
1450	0.75	Zirconolite	45	2	14	14	78	34
		Perovskite	55	98	86	86	22	66

The ceramic with x = 0.75 sintered at 1450 ^{0}C is composed of major dark-gray colored (on SEM-image) bulk formed by aggregates of sub-micron grains of the perovskite-type and zirconolite phases (Figure 4). Approximate calculated formulae of zirconolite and perovskite (in suggestion

that all Zr enters zirconolite are as follows: $Ca_{0.17}Gd_{0.90}Zr_{1.00}Ti_{1.17}Al_{0.76}O_7$ and $Ca_{0.38}Gd_{0.70}Ti_{0.38}Al_{0.54}O_3$. Light-gray fianite inclusions with averaged formula $Zr_{0.67}Ti_{0.06}Gd_{0.21}Ca_{0.03}O_{1.805}$ are distributed in the major bulk.

As seen from Table II major host phase for all the elements in the Eu-bearing ceramics at x = 0.25 is zirconolite as predominant phase. At x = 0.5 it remains the major phase for all elements except calcium which is equally partitioned between zirconolite and perovskite. In the Gd-bearing ceramics as well as in the systems with neodymium, samarium [14], and europium oxides major host phase for Gd and Zr at x = 0.25 and x = 0.5 is zirconolite (Table II). Fraction of their oxides incorporated by perovskite grows with the increase of x value. Behavior of other oxides in the given system is similar to their behavior in the Nd-, Sm- [14], and Eu-bearing ceramics.

XRD pattern of the zirconolite (Figures 1 and 3) corresponds with high probability to trigonal variety (zirconolite-3T) as it is seen from absence of some superstructure reflections typical of the monoclinic symmetry zirconolite-2M lattice. Unit cell parameters of the zirconolite-3T calculated from XRD data are given in Table III. No rigorous correlation between unit cell parameters and synthesis conditions and chemical composition of the zirconolite phase was found due to several reasons: deviation of lattice symmetry from trigonal, incomplete equilibrium in the systems under the given synthesis conditions (temperature and sintering time), co-existence of Eu in both di- and trivalent forms, etc. To determine lattice symmetry of the zirconolite phase more precisely additional electron diffraction investigation is required.
It should be also noted, that the zirconolite phase in the Eu- and Gd-bearing ceramics is predominant or at least exists in much broad compositional range than in Nd-, Sm-, and particularly La-bearing ceramics due to much higher isomorphic capacity of zirconolite with respect to Eu and Gd (>1 fu). Isomorphic capacity of zirconolite with respect to lanthanides increases from La to Gd (zirconolites with Y-group lanthanides are studied insufficiently). As it has been shown in one of our previous works [10] Ca-free REE-substituted zirconolites $TRZrTiAlO_7$ are formed with Pr and heavier lanthanides but in the Pr-, Nd-, and Sm-bearing systems along with Ca-free zirconolite extra phases were present as well, whereas no extra phases were found in the Gd-bearing system. Since the key problem is immobilization of the most dangerous actinide fraction of HLW, containing mainly trivalent Am and Cm, whose crystal chemical behavior is similar to that of Gd, in amount of about 0.1 kg per metric tonne of spent nuclear fuel [1] ceramization of this fraction may yield almost monophasic zirconolite ceramics. High chemical durability and radiation resistance of zirconolite have been proven by numerous investigations of both synthetic and naturally-occurred samples containing U, Th, and their daughter products [2,3,6,16,17].

CONCLUSION

Ceramics related to pseudo-binary systems: zirconolite – lanthanide aluminate (perovskite) in the series (1-x) $CaZrTi_2O_7$ – x $EuAlO_3$ and (1-x) $CaZrTi_2O_7$ – x $GdAlO_3$ (x = 0.25, 0.5 and 0.75) sintered at 1400, 1450, and 1500 ^{0}C at x = 0.25 and 0.5 are composed of zirconolite (trigonal variety) and perovskite. With increase of x value zirconolite content reduces whereas perovskite content increases. At x = 0.75 extra oxide fianite-type phase occurs, perovskite becomes major phase and zirconolite content becomes comparable with fianite. At x = 0.25 zirconolite is major

host phase for most of elements, in particular it accumulates almost all Zr and ~90% Eu and Gd. At x = 0.75 fraction of Eu and Gd incorporated in zirconolite reduces to about 34% of total.

Table III. Unit Cell Parameters of Trigonal Zirconolite-3T phase in ceramics.

Dopant	T, ^{0}C	*x*, f.u..	*a*, Å	*b,* Å	*c,* Å	∠*β*, deg.	Formula
Eu	1400	0.25	7.240	7.240	16.752	90.00	-
		0.5	7.255	7.255	16.728	90.00	-
		0.75	7.282	7.282	16.752	90.00	-
	1450	0.25	7.233	7.233	16.728	90.00	$Ca_{0.76}Eu_{0.30}Zr_{1.04}Ti_{1.63}Al_{0.27}O_7$
		0.5	7.247	7.247	16.728	90.00	-
		0.75	7.277	7.277	16.734	90.00	$Ca_{0.44}Eu_{1.52}Zr_{0.58}Ti_{0.70}Al_{0.76}O_{6.42}$
	1500	0.25	7.227	7.227	16.728	90.00	-
		0.5	7.248	7.248	16.752	90.00	$Ca_{0.46}Eu_{0.64}Zr_{1.16}Ti_{1.28}Al_{0.47}O_7$
		0.75	7.269	7.269	16.740	90.00	-
Gd	1400	0.25	7.237	7.237	16.710	90.00	-
		0.5	7.249	7.249	16.692	90.00	-
		0.75	7.259	7.259	16.674	90.00	-
	1450	0.25	7.222	7.222	16.680	90.00	$Ca_{0.72}Gd_{0.28}Zr_{1.00}Ti_{1.68}Al_{0.28}O_7$
		0.5	7.251	7.251	16.698	90.00	$Ca_{0.26}Gd_{0.98}Zr_{1.04}Ti_{1.08}Al_{0.68}O_7$
		0.75	7.270	7.270	16.716	90.00	$Ca_{0.17}Gd_{0.90}Zr_{1.00}Ti_{1.17}Al_{0.76}O_7$
	1500	0.25	7.233	7.233	16.722	90.00	-
		0.5	7.243	7.243	16.698	90.00	$Ca_{0.41}Gd_{0.61}Zr_{1.15}Ti_{1.29}Al_{0.53}O_7$
		0.75	7.279	7.279	16.758	90.00	-

ACKNOWLEDGEMENT

Authors thank Mr. Boris Nikonov (IGEM RAS) for his help in SEM/EDS study of ceramics.

REFERENCES

1. A.V. Ochkin, N.S. Babaev, E.P. Magometbekov, "Introduction to Radioecology," Moscow (2003).
2. E.C. Buck, B. Ebbinghaus, A.J. Bakel, J.K. Bates, "Characterization of a Plutonium-Bearing Zirconolite-Rich Synroc," Mat. Res. Soc. Symp. Proc. **465** (1997) 1259-1266.
3. B.B. Ebbinghaus, R.A. Vankonynenburg, F.J. Ryerson, E.R. Vance, M.W.A. Stewart, A. Jostsons, J.F. Allender, T. Rankin, J. Congdon, "Ceramic Formulation for the Immobilization of Plutonium," Proc. Int. Symp. Waste Management '98. Tucson, AZ, 1998. Rep. 65-04. CD-ROM.
4. E.R. Vance, M.L. Carter, B.D. Begg, R.A. Day, S.H.F. Leung, "Solid Solubilities of Pu, U, Hf and Gd in Candidate Ceramic Phases for Actinide Waste Immobilization," Mat. Res. Soc. Symp. Proc. **608** (2000) 431-436.
5. S.V. Stefanovsky, S.V. Yudintsev, B.S. Nikonov, A.V. Ochkin, S.V. Chizhevskaya, N.E. Cherniavskaya, "Phase Composition and Elements Partitioning in Two-Phase Hosts for

Immobilization of a Rare Earth – Actinide High-Level WasteFraction," Mat. Res. Soc. Symp. Proc. **608** (2000) 407-412.
6. E.R. Vance, A. Jostsons, R.A. Day, C.J. Ball, B.D. Begg, P.J. Angel, "Excess Pu Disposition in Zirconolite-Rich Synroc," Mat. Res. Soc. Symp. Proc. **412** (1996) 41-47.
7. S.V. Stefanovsky, A.Y. Troole, M.I. Lapina, B.S. Nikonov, A.V. Sivtsov, S.V. Yudintsev, "XRD, SEM and TEM Study of the Gd-Doped Zirconolites," Mat. Res. Soc. Symp. Proc. **713** (2002) 345-350.
8. S.V. Stefanovsky, S.V. Chizhevskaya, A.S. Mironov, "Phase Composition of Gadolinium-Containing Zirconolite Ceramics Synthesized by Cold Pressing and Sintering Method from Mechanically Activated Oxide Batch," Phys. Chem. Mater. Treat. (Russ.) [4] (2003) 85-91.
9. S.V. Stefanovsky, S.V. Yudintsev, B.S. Nikonov, A.S. Mironov, "Incorporation of Corrosion Products in Gadolinium-Substituted Zirconolite," Phys. Chem. Mater. Treat. (Russ.) [6] (2003) 83-88.
10. S.V. Stefanovsky, S.V. Chizhevskaya, A.S. Mironov, O.I. Kirjanova, S.V. Yudintsev," Adv. Mater. (Russ.) [6] (2003) 61-68.
11. E.R. Vance, R.A. Day, Z. Zhang, B.D. Begg, C.J. Ball, M.G. Blackford, "Charge Compensation in Gd-Doped $CaTiO_3$," J. Solid State Chem. **124** (1996) 77-82.
12. O.I. Kirjanova, A.V. Ochkin, S.V. Stefanovsky, N.E. Cherniavskaya, "Phase Composition of Ceramics in System CaO-La_2O_3-Al_2O_3-TiO_2-ZrO_2 Produced by Cold Pressing and Sintering at 1350-1550 ^{0}C," Adv. Mater. (Russ.) [4] (2001) 17-23.
13. N.S. Mikhailenko, S.V. Stefanovsky, A.V. Ochkin, "Phase Relations and Elemental Distribution among Co-Existing Phases in the Ceramics of the Pseudo-Binary System $CaZrTi_2O_7$ – $CeAlO_3$," Proc. Waste Management '06 Conf. Tucson, AZ, February 26 – March 2, 2006. CD-ROM. ID 6592. 10p.
14. N.S. Mikhailenko, S.V. Stefanovsky, A.V. Ochkin, "Phase Relations and Distribution of Elements in Ceramics of Pseudobinary Systems $CaZrTi_2O_7$-$LnAlO_3$ (Ln=Nd,Sm)," Human Ecology and the Nature. Proc. 6th Intern. Conf. (Russ.) Moscow-Ples (2004) 62-66.
15. N.S. Mikhailenko, A.V. Ochkin, S.V. Stefanovsky, O.I. Kirjanova, "Phase Relations and Chemical Durability of Ceramics in the Pseudo-Binary System: $CaZrTi_2O_7$-$GdAlO_3$," Mat. Res. Soc. Symp. Proc. **807** (2004) 327-332.
16. A.E. Ringwood, S.E. Kesson, K.D. Reeve, D.M. Levins, E.J. Ramm, "Synroc," Radioactive Waste Forms for the Future. Eds W. Lutze and R.C. Ewing. Amsterdam: Elsevier Science Publishers B.V., 1988, p. 233-334.
17. W.J. Weber, R.C. Ewing, C.R.A. Catlow, T. Diaz De La Rubia, L.W. Hobbs, C. Kinoshita, Hj. Matzke, A.T. Motta, M. Nastasi, E.K.H. Salje, E.R. Vance, S.J. Zinkle, "Radiation Effects in Crystalline Ceramics for the Immobilization of High-Level Nuclear Waste and Plutonium," J. Mat. Res. **13** (1998) 1434-1484.